25 May 2000

ELSEVIER

Optics Communications 179 (2000) 559–570

OPTICS COMMUNICATIONS

www.elsevier.com/locate/optcom

Recoil-induced effects in passive and active atomic systems

R. Bonifacio [a], B.W.J. McNeil [b], N. Piovella [a], G.R.M. Robb [b,*]

[a] *Dipartimento di Fisica, Universitá Degli Studi di Milano, INFN & INFM, Via Celoria 16, I-20133 Milano, Italy*

[b] *Department of Physics and Applied Physics, John Anderson Building, University of Strathclyde, Glasgow G4 0NG, Scotland, UK*

Received 16 August 1999; received in revised form 20 September 1999; accepted 22 September 1999

Abstract

A theoretical analysis of absorptive optical bistability in a passive atomic medium and bidirectional lasing in an active atomic medium is presented. The atomic medium consists of a collection of cold two-level atoms and the atom-radiation field interaction is described using a one-dimensional semiclassical model. It is shown that when the effects of atomic recoil are included self-consistently, the interaction between the atoms and the radiation can be changed significantly from that when the effects of atomic recoil are neglected.

1. Introduction

Until recently, the role of atomic recoil in optical physics was generally considered to be a minor one. However, with the continuing progress in optical cooling and trapping of atomic vapours demonstrating the mechanical effects of light on atomic dynamics and the recent interest in optical phenomena which can be directly related to atomic recoil e.g. the collective atomic recoil laser (CARL) [1–3] and recoil-induced resonances [4–6], this is no longer true.

In this paper, we present a theoretical analysis of two well-known phenomena in optical physics: absorptive optical bistability (OB) in a passive (non-inverted) atomic medium and bidirectional lasing in an active (inverted) atomic medium, using a semiclassical, one-dimensional model. Some of the material on absorptive OB appears elsewhere but is included here for completeness. In contrast to previous theoretical analyses of these effects, the atomic medium is assumed to consist of a collection of cold two-level atoms, and the effects of recoil are described self-consistently i.e. in addition to describing the mechanical effects of the radiation fields on the atomic internal and external (centre-of-mass) dynamics, the model also describes the back-action of the ensemble of atoms on the radiation fields.

It is shown that when the effects of atomic recoil are treated self-consistently, it is possible for the nature of the interaction between the two-level atoms and the radiation to be changed significantly from that when atomic recoil is neglected: for absorptive OB, when the effects of atomic recoil are included, the low-transmission regime of the system is unstable. This instability simultaneously generates an atomic density grating and a radiation field coherently back-scattered by it from the incident pump field. The formation of the density grating is induced by a modulated potential resulting from the interfer-

* Corresponding author. E-mail: g.r.m.robb@strath.ac.uk

0030-4018/00/$ - see front matter
PII: S0030-4018(99)00544-1

ence of the scattered and incident fields. The modulation is a consequence of the nonlinear absorption of the atoms in the standing wave produced by the counterpropagating radiation fields which induces a population difference grating with a period of half the radiation wavelength. The effects of the additional back-scattered field and the density grating are shown to have a significant influence on the bistable properties of the system. For the ring laser, it is well known that, neglecting atomic recoil, the bidirectional lasing solution is unstable in the absence of Doppler broadening and the system exhibits a bistable behavior with unidirectional emission in one direction or the other, depending on the initial conditions. When the effects of atomic recoil are included, the average atomic momentum induced by radiation pressure affects the stability of the steady-state lasing: when the cavity modes are resonant with the atomic frequency, the bidirectional solution becomes stable. Detuning the cavity mode above resonance, periodic unidirectional lasing in opposite directions is observed, whereas below resonance lasing is suppressed in both directions.

2. Model

A schematic of the ring cavity system considered here is shown in Fig. 1. The atoms may be excited by some external incoherent energy source (not shown). The model used to describe the interaction is one-dimensional and semiclassical. The internal atomic dynamics (dipole moment and population difference) are described as a quantum-mechanical

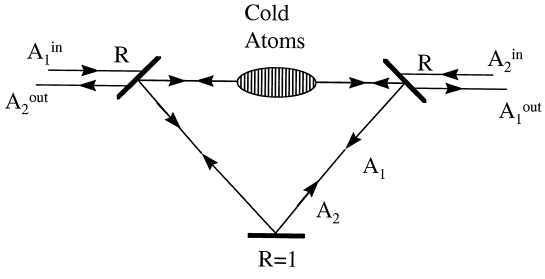

Fig. 1. A schematic diagram showing a cold atomic sample enclosed in a bidirectional ring cavity. Note that $A_{1,2}^{eq} = A_{1,2}^{in}/\sqrt{1-R}$ and $A_{1,2}^{out} = A_{1,2}\sqrt{1-R}$ where R is the reflectivity of the output mirrors.

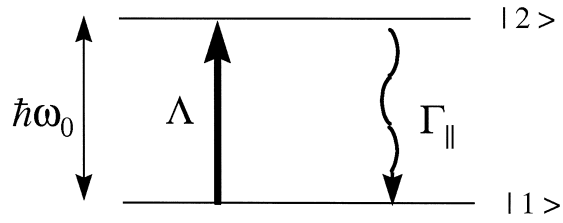

Fig. 2. A schematic energy level diagram of the atoms.

two-level system and the external atomic dynamics (position and momentum) are treated classically, with the atoms as point particles. The atoms in our model are assumed to be 'cold', by which we mean that their temperature is sufficiently low that Doppler broadening effects can be neglected [2]. For temperatures of the order of the recoil temperature of the atoms or less, the wave nature of the atoms becomes significant and their centre-of-mass motion must also be treated quantum-mechanically [3].

We now outline the derivation of the set of equations used to describe the atom-field interaction within the cavity. These equations extend the so-called Maxwell–Bloch model [7] to self-consistently include the atomic centre-of-mass motion and can describe a wide range of radiation-atom interactions.

We define the counterpropagating probe and pump radiation electric fields as

$$\boldsymbol{E}(z,t) = \left(\mathscr{E}_1(z,t)\mathrm{e}^{\mathrm{i}(k_1 z-\omega_1 t)} + \mathscr{E}_2(z,t)\mathrm{e}^{-\mathrm{i}(k_2 z+\omega_2 t)} + \mathrm{c.c.}\right)\hat{\boldsymbol{e}},$$

where $\hat{\boldsymbol{e}}$ is a unit vector transverse to the propagation axis $\hat{\boldsymbol{z}}$ and subscripts 1,2 refer to the probe and pump respectively. The energy level diagram for each atom in the sample is shown in Fig. 2. The evolution of the density matrix elements $\rho_{mn},(m,n=1,2)$ describe the internal evolution of each atom. The off-diagonal elements ($\rho_{21} = \rho_{12}^*$) describe the polarisation as induced by the pump and the probe fields. The dipole moment is then given by

$$\boldsymbol{d} = \mu(\rho_{12} + \rho_{12}^*)\hat{\boldsymbol{e}}, \tag{1}$$

where μ is the dipole matrix element. The off-diagonal elements in Eq. (1) may be written conveniently as a sum of two polarisation waves

$$\rho_{12} = S_1(z,t)\mathrm{e}^{\mathrm{i}(k_1 z-\omega_1 t)} + S_2(z,t)\mathrm{e}^{-\mathrm{i}(k_2 z+\omega_2 t)} \tag{2}$$

and we define D as half the population difference between the lower (1) and upper (2) states, so that

$$D = \frac{\rho_{11} - \rho_{22}}{2}.$$

Use of the definitions above in the Bloch equations describing the two-level atomic system, the equation for the force on the jth atom

$$F_{z_j} = \left(\boldsymbol{d} \cdot \frac{\partial \boldsymbol{E}}{\partial z} \right)\Bigg|_{z=z_j},$$

and the Maxwell wave equation yield the following set of coupled scaled differential equations, which in the limit of no incoherent excitation ($\Lambda = 0$), reduce to those of [8]:

$$\frac{\mathrm{d}\tilde{S}_{1_j}}{\mathrm{d}\tau} = \left[-\Gamma_\perp + \mathrm{i}\left(\Delta - \frac{p_j}{2} \right) \right] \tilde{S}_{1_j} - 2\rho \tilde{A}_1 D_j, \tag{3}$$

$$\frac{\mathrm{d}S_{2_j}}{\mathrm{d}\tau} = \left[-\Gamma_\perp + \mathrm{i}\left(\Delta + \frac{p_j}{2} \right) \right] S_{2_j} - 2\rho A_2 D_j, \tag{4}$$

$$\frac{\mathrm{d}D_j}{\mathrm{d}\tau} = -(\Gamma_\parallel + \Lambda)\left(D_j - D^{\mathrm{eq}} \right) + \rho\left[\tilde{S}_{1_j}\left(\tilde{A}_1^* + A_2^* \mathrm{e}^{\mathrm{i}\theta_j} \right) + S_{2_j}\left(\tilde{A}_1^* \mathrm{e}^{-\mathrm{i}\theta_j} + A_2^* \right) + \mathrm{c.c.} \right], \tag{5}$$

$$\frac{\mathrm{d}\theta_j}{\mathrm{d}\tau} = p_j, \tag{6}$$

$$\frac{\mathrm{d}p_j}{\mathrm{d}\tau} = -\left(\tilde{A}_1 \tilde{S}_{1_j}^* - A_2 S_{2_j}^* + \tilde{A}_1 S_{2_j}^* \mathrm{e}^{\mathrm{i}\theta_j} - A_2 \tilde{S}_{1_j}^* \mathrm{e}^{-\mathrm{i}\theta_j} + \mathrm{c.c.} \right), \tag{7}$$

$$\frac{\mathrm{d}\tilde{A}_1}{\mathrm{d}\tau} = \left\langle \tilde{S}_1 \right\rangle + \left\langle S_2 \mathrm{e}^{-\mathrm{i}\theta} \right\rangle + \mathrm{i}\delta \tilde{A}_1 - \kappa_1\left(\tilde{A}_1 - \tilde{A}_1^{\mathrm{eq}} \right), \tag{8}$$

$$\frac{\mathrm{d}A_2}{\mathrm{d}\tau} = \left\langle S_2 \right\rangle + \left\langle \tilde{S}_1 \mathrm{e}^{\mathrm{i}\theta} \right\rangle - \kappa_2\left(A_2 - A_2^{\mathrm{eq}} \right), \tag{9}$$

where the general dependent variables $X \equiv X(\tau)$, $\tilde{X} \equiv X \mathrm{e}^{\mathrm{i}\delta\tau}$ and

$$A_{1,2} = -\mathrm{i}\sqrt{\frac{2\epsilon_0}{n\hbar\omega\rho}}\,\mathscr{E}_{1,2}, \quad \rho = \left(\frac{\omega\mu^2 n}{2\epsilon_0 \omega_r^2 \hbar} \right)^{1/3},$$

$$p = \frac{M\left(v_z - \langle v_{z0} \rangle \right)}{\hbar k \rho}, \quad \Delta = \frac{\omega_2 + k_2 \langle v_{z0} \rangle - \omega_0}{\omega_r \rho},$$

$$\delta = \frac{2k\langle v_{z0} \rangle - (\omega_1 - \omega_2)}{\omega_r \rho},$$

$\tau = \omega_r \rho t$, $\theta = 2k(z - \langle v_{z0} \rangle t)$, $\omega_r = 2\hbar k^2/M$ is the single photon recoil frequency shift, $j = 1, \ldots, N$, $\langle \ldots \rangle = \frac{1}{N}\sum_{j=1}^{N}(\ldots)$ and $\Gamma_{\perp,\parallel} = \gamma_{\perp,\parallel}/\omega_r \rho$ are the scaled decay rates of the polarisation and upper level population respectively. In the above scaling, M is the atomic mass, ω_0 is the transition frequency, $n = n_s L_s / L_{\mathrm{cav}}$ is the 'reduced' atomic density in the cavity, n_s is the atomic density of the sample, L_s is the sample length, L_{cav} is the cavity length and where appropriate we have assumed $k \approx (k_1 + k_2)/2$. Note that for an atomic sample which initially has zero mean velocity ($\langle v_{z0} \rangle = 0$), $\Delta \to (\omega_2 - \omega_0)/\omega_r \rho$ and $\delta \to (\omega_2 - \omega_1)/\omega_r \rho$. Hence Δ and δ describe the pump-atom detuning and the pump-probe detuning respectively, scaled with respect to the 'collective recoil bandwidth', $\omega_r \rho$ [1,2]. In this paper, we consider only cases where the frequencies of the two fields are equal i.e. $\omega_1 = \omega_2$ and $\langle v_{z0} \rangle = 0$, so $\delta = 0$ is assumed throughout. In deriving Eqs. (3)–(9), the pump and probe fields are assumed to be average fields over intervals $\Delta z \sim \lambda$, the radiation wavelength, consistent with the slowly varying envelope approximation (SVEA) [7]. The mean, $\langle \ldots \rangle$, refers to the N atoms within that interval.

We have assumed that the mean field limit can be applied when describing the evolution of both the pump and the probe. Cavity losses are assumed to be equal for both pump and probe i.e. $\kappa_1 = \kappa_2 = \kappa$, where $\kappa = -c\ln(R)/\omega_r \rho L_{\mathrm{cav}}$ is the scaled cavity loss rate. Here $\tilde{A}_1^{\mathrm{eq}}$ and A_2^{eq} are the constant probe and pump fields input to the cavity. It has been assumed that the pump frequency coincides with that of a mode of the cavity i.e. $\omega_2 = \omega^{(m)} = 2\pi m c / L_{\mathrm{cav}}$ where m is an integer.

The distinction between a passive and active atomic system arises from D^{eq}, the equilibrium value of D in the absence of the radiation fields, defined as

$$D^{eq} = \frac{1}{2}\left(\frac{\Gamma_{\parallel} - \Lambda}{\Gamma_{\parallel} + \Lambda}\right). \tag{10}$$

Consequently, in the absence of excitation ($\Lambda = 0$), $D^{eq} = 0.5$, the atoms relax to their ground state and the atomic medium is passive. In contrast, for strong excitation ($\Lambda \gg \Gamma_{\parallel}$) $D^{eq} \approx -0.5$, the atoms relax to the upper state and the atomic system is inverted or active.

3. Passive atomic system: absorptive optical bistability

3.1. Introduction

An optical system which exhibits two steady transmission states for the same input intensity is said to be optically bistable. In this section we investigate optical bistability (OB) of an absorbing system of cold, two-level atoms enclosed in a bidirectional ring cavity. In contrast to previous analyses of absorptive OB [9–11] we include the effects of atomic recoil.

To the authors' knowledge, previous works have only approximated the effects of atomic motion through an inhomogeneous broadening of the atomic transition. Such thermal effects do not require a detailed description of the atomic positions and momenta. It is shown that when the effects of atomic recoil are included self-consistently, the bistable behaviour of the ring cavity system is changed significantly.

3.2. Model

The experimental setup we describe is shown schematically in Fig. 1. We assume that there is no incoherent excitation of the atomic system ($\Lambda = 0$), so $D^{eq} = 0.5$ and the atomic medium is passive. For simplicity, we assume $\Gamma_{\perp} = \Gamma_{\parallel} \equiv \Gamma$. The atoms are assumed to be cold initially and momentum diffusion due to spontaneous emission is neglected. We return to the issue of momentum diffusion later in the paper where we derive the condition for which it can be neglected.

3.3. Absorptive optical bistability neglecting recoil

We now use the model described in Sections 2 and 3.2 to demonstrate the well-known phenomenon of absorptive optical bistability in the absence of atomic recoil and for a unidirectional ring cavity. To do this, we set $d\theta/d\tau = dp/d\tau = \tilde{A}_1 = \tilde{S}_1 = 0$. It can be shown that the resulting Eqs. (4), (5) and (9) have bistable solutions when the condition $C > 4$ is satisfied, where $C = \rho/2\kappa\Gamma$ is the cooperation parameter [11]. Optical bistability is demonstrated in the usual way in Fig. 3 by plotting the scaled field amplitude $|A_2|$ as a function of the scaled input field amplitude $|A_2^{eq}|$ for $C = 25$. We will use this example to study the stability of the solutions when atomic motion is included in the model.

3.4. Recoil-induced instability

The restrictions in Section 3.3 are now relaxed and we consider the general case of a bidirectional ring cavity including the effects of atomic recoil. We investigate the stability of the solutions for A_2 on the lower branch of the bistability curve of Fig. 3 for small initial values of A_1 and a cold atomic sample.

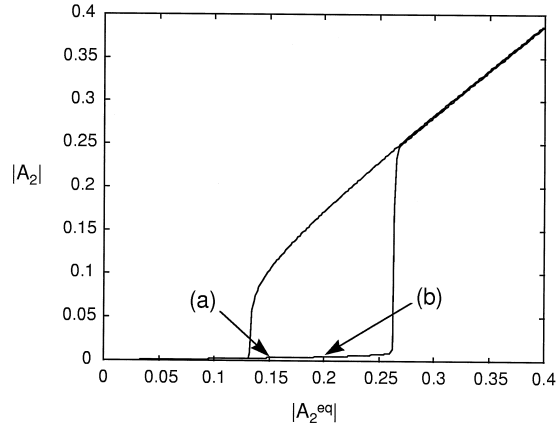

Fig. 3. Absorptive OB: Pump field amplitude $|A_2|$ in the cavity as a function of the injected pump field amplitude $|A_2^{eq}|$ for $\rho = 1500$, $\kappa = 1$, $\Gamma = 30$ and $\Delta = 0$ giving a cooperation parameter $C = 25$.

An equilibrium value A_2^{eq} and initial value of A_2 close to the steady-state solution for A_2 is taken from the lower branch of Fig. 3. The system of Eqs. (3)–(9) is then integrated numerically.

The behaviour of the system was investigated for different values of A_2^{eq} and $A_2(\tau = 0)$ corresponding to points lying close to the lower branch of Fig. 3.

The solution of Eqs. (3)–(9) are shown in Figs. 4 and 5. Fig. 4 shows the evolution of $|A_2|^2$, $|A_1|^2$ and the atomic bunching parameter $|b|$ for conditions corresponding to point (a) on Fig. 3. It can be seen that $|A_1|^2$ and $|b|$ display exponential growth, but when $|A_1|^2 \approx |A_2|^2$ the value of $|A_2|^2$ undergoes a sudden transition to a larger value before returning to its approximately constant value which is very close to that when atomic motion is neglected.

Fig. 5 shows the evolution of $|A_1|^2$ and $|A_2|^2$ and the bunching parameter $|b|$ for conditions corresponding to point (b) on Fig. 3. The bunching parameter $b = \langle e^{-i\theta} \rangle$ is a measure of the spatial distribution of the atoms on the wavelength scale ($b = 0$ for a uniform distribution of θ_j and $|b| = 1$ when $\theta_j = \text{constant} \forall j$). The behaviour of $|b|$ shown in Figs. 4 and 5 indicates that the initially uniformly distributed atoms become strongly bunched on a scale of $\lambda/2$. A physical mechanism for this bunching is described in Section 3.5. In this case, when $|A_1|^2$ grows to become approximately equal to $|A_2|^2$,

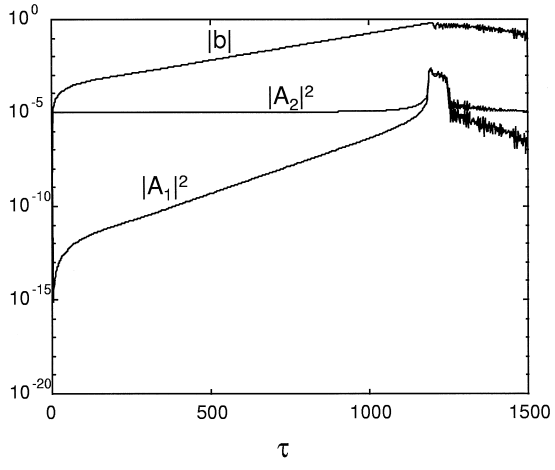

Fig. 4. Absorptive OB: Evolution of the probe intensity $|A_1|^2$, pump intensity $|A_2|^2$ and bunching parameter amplitude $|b|$ in the cavity as a function of scaled time τ for $A_2^{eq} = 0.15$, $A_1^{eq} = 0, \rho = 1500$, $\kappa = 1$, $\Gamma = 30$ and $\Delta = 0$.

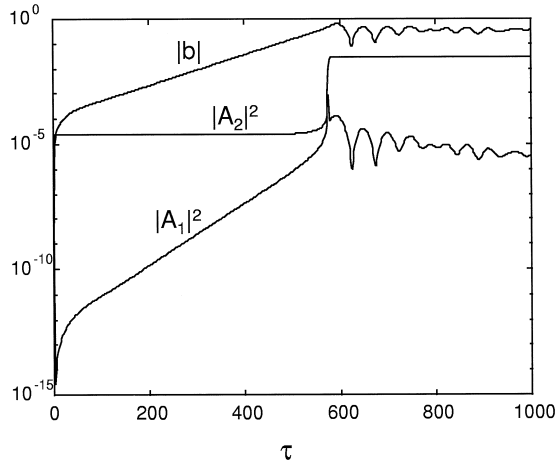

Fig. 5. Absorptive OB: Evolution of the probe intensity $|A_1|^2$, pump intensity $|A_2|^2$ and bunching parameter amplitude $|b|$ in the cavity as a function of scaled time τ for $A_2^{eq} = 0.2$, $A_1^{eq} = 0$, $\rho = 500$, $\kappa = 1$, $\Gamma = 30$ and $\Delta = 0$. Switching of the pump to the high transmission state occurs at $\tau \approx 550$.

$|A_2|^2$ undergoes a sudden transition to a higher steady-state value. This steady-state for $|A_2|$ is approximately equal to the upper branch of the bistable curve on Fig. 3. Therefore it has been shown that for a sufficiently large value of $|A_2^{eq}|$, the lower branch of the bistability curve for 'fixed' atoms in a unidirectional ring cavity becomes unstable when an additional counter-propagating wave is introduced and the atomic centre-of mass motion is included. Note that this counter-propagating wave can arise from noise in the system. That this instability is intimately linked to atomic motion and not just due to induced effects in stationary atoms can be shown by setting $d\theta/d\tau = dp\, d\tau = 0$ in Eqs. (3)–(9) while letting S_1 and A_1 evolve. When this is carried out, $|A_1|$ does not deviate from its initially small value and $|A_2|$ attains a steady-state value equal to that when atomic motion is neglected and the evolution of A_1 is suppressed (Fig. 3).

3.5. Analysis

In this section we show how two counter-propagating fields resonant with an ensemble of two-level atoms can produce a force which acts to spatially bunch the atoms. If we assume for simplicity that the atomic momentum is sufficiently small that $p \ll \Gamma$,

and that $\Gamma \gg \kappa$, it is possible to adiabatically eliminate the 'internal' atomic variables S_1, S_2 and D for the jth atom and solve for D_j. If we assume weak nonlinearity ($4\rho^2|A_{1,2}|^2 \ll \Gamma^2$) then the result is

$$D_j \approx \frac{1}{2}\left[1 - \frac{4\rho^2}{\Gamma^2} I(\theta_j)\right], \tag{11}$$

where

$$I(\theta) = |A_1|^2 + |A_2|^2 + A_1 A_2^* e^{i\theta} + A_1^* A_2 e^{-i\theta}$$

is the total scaled intensity due to the interference of the probe and pump fields. For the case where the atoms are uniformly distributed in space, it can be seen from Eq. (11) that the population difference contains a sinusoidal variation due to the modulated intensity $I(\theta)$. We now show that this 'population difference grating' can give rise to a bunching force by substituting for S_1, S_2 and D in the force Eq. (7) using (11), which produces

$$\frac{dp_j}{d\tau} = \frac{2\rho}{\Gamma}\left(|A_1|^2 - |A_2|^2\right)\left[1 - \frac{4\rho^2}{\Gamma^2} I(\theta_j)\right]. \tag{12}$$

The first term in Eq. (12) is the usual radiation pressure force, which is position (θ) independent. The second term in Eq. (12) describes a reduction in the radiation pressure force due to nonlinear 'bleaching' of the atoms' response to the field. Note that this bleaching is position dependent, giving rise to a force which is modulated with the radiation intensity that the atoms experience. It is this modulated force which acts to bunch the atoms in space to form a density grating.

If we now assume that $|A_2|$ is constant and A_1, b and p are small quantities, it can be shown from a linear analysis of Eqs. (3)–(8) using the method of collective variables [12] that both $A_1, b \propto e^{\lambda t}$ and therefore both will grow exponentially if the cubic

$$\lambda^3 + \left(\frac{\rho}{\Gamma} + \kappa\right)\lambda^2 + \frac{i}{2}\left(\frac{\Omega}{\Gamma}\right)^4\left(\frac{\lambda}{2\Gamma} - 1\right) = 0 \tag{13}$$

has any solutions with $\mathrm{Re}(\lambda) > 0$. It can be shown that

$$\Re(\lambda) \approx \frac{\Omega^2}{\Gamma^2}\frac{1}{2\sqrt{\left(\kappa + \frac{\rho}{\Gamma}\right)}}, \tag{14}$$

where $\Omega = 2\rho|A_2|$ is the scaled pump Rabi frequency, so $\mathrm{Re}(\lambda) > 0$ always.

3.6. Momentum diffusion due to spontaneous emission

The results obtained in the previous sections were derived using a model which neglects the influence of momentum diffusion due to spontaneous emission. In this section we derive the condition which must be satisfied in order to neglect the effects of momentum diffusion.

Atoms undergoing spontaneous emission emit photons in random directions. Consequently, the atoms feel randomly directed momentum 'kicks' of magnitude $\hbar k$. The long term effect of this is to cause a random walk in momentum space. For simplicity, we consider the effect of spontaneous emission as a one-dimensional random walk. N spontaneous emission events correspond to N momentum 'steps' of magnitude $\hbar k$. This gives rise to an atomic momentum spread [13] of

$$\left\langle (Mv)^2 \right\rangle \approx N(\hbar k)^2 = \hbar^2 k^2 \rho_{22} \gamma t \tag{15}$$

as $N = \gamma\rho_{22} t$, where ρ_{22} is the probability of finding an atom in the upper energy state $|2\rangle$. In the scaled notation of this paper, (15) can be expressed as

$$\langle p^2 \rangle \approx 2 D_p \tau, \tag{16}$$

where $D_p = \Gamma\rho_{22}/2\rho^2$ is the scaled diffusion coefficient.

The effect of atomic momentum spread is to cause the amplitude of the density grating, described by $|b|$, to decay. In order to neglect the effects of momentum diffusion, the decay of the grating due to the induced atomic momentum spread must be negli-

gible during the growth of the density grating due to the instability. In order to determine the condition under which this is possible, we follow a similar approach to that of [2].

Let us assume that at $t = 0$ the atoms are perfectly bunched on the scale of $\lambda/2$, so that they have the same value of θ (taken to be zero) and $|b| = 1$. Letting the atoms evolve under the action of spontaneous emission, the bunching at time τ can be determined by writing the bunching factor b in the form

$$b(\tau) = \int_{-\infty}^{\infty}\int_{-\infty}^{\infty} f(\theta, p, \tau)\mathrm{e}^{-\mathrm{i}\theta}\mathrm{d}\theta\,\mathrm{d}p, \tag{17}$$

where $f(\theta, p, \tau)$ is the probability of finding an atom with a scaled position in the interval $\theta \to \theta + \mathrm{d}\theta$ and scaled momentum in the interval $p \to p + \mathrm{d}p$ at time τ. Assuming that both the distribution in θ and p are Gaussian, then we can write

$$f(\theta, p, \tau) = \frac{\exp\left(\dfrac{-\theta^2}{2\sigma_\theta(\tau)^2}\right)}{\sqrt{2\pi}\,\sigma_\theta(\tau)} \frac{\exp\left(\dfrac{-p^2}{2\sigma_p(\tau)^2}\right)}{\sqrt{2\pi}\,\sigma_p(\tau)}, \tag{18}$$

where in accordance with Eq. (16),

$$\sigma_p(t) = \sqrt{2D_p\tau}, \tag{19}$$

$$\sigma_\theta = \int_0^\tau \sigma_p(\tau')\mathrm{d}\tau' = \frac{2\sqrt{2D_p}}{3}\tau^{3/2}. \tag{20}$$

Substituting (18)–(20) in (17) we obtain

$$b(\tau) = \exp\left(-\frac{4D_p\tau^3}{9}\right). \tag{21}$$

The condition for the neglect of momentum diffusion due to spontaneous emission is then $4D_p\tau_g^3/9 \ll 1$ or

$$\frac{\Gamma}{9\rho^2}\frac{\Omega^2}{(\Gamma^2 + \Omega^2)}\tau_g^3 \ll 1, \tag{22}$$

where the relation $\rho_{22} = \Omega^2/2(\Gamma^2 + \Omega^2)$ has been used and τ_g is the characteristic growth time of the density grating due to the instability. From Fig. 5, it can be seen that $\tau_g \approx 70$ and $|A_2| \approx 0.0048$, so for the parameters used in Fig. 5, the LHS of (22) is approximately 0.095. The neglect of momentum diffusion due to spontaneous emission in this example is therefore consistent with the physical arguments described above.

4. Active atomic system: the bidirectional ring laser

4.1. Introduction

When the two-level atomic system shown in Fig. 2 is strongly pumped by some external energy source, so that $D^{\mathrm{eq}} < 0$, the atomic medium becomes active and we have a simple model of a laser system. Bidirectional ring lasers have been studied for many years [14], in large part due to their application as laser gyroscopes. It is well known [15] that a homogeneously broadened ring laser admits two stationary solutions, a standing wave oscillation formed by two counterpropagating modes of equal intensity and a travelling wave oscillation consisting of a single-mode propagating in one direction. The coupling between the two modes is provided by the scattering from the spatial grating formed in the population difference. The bidirectional solution is unstable and the unindirectional solution is stable if the cavity decay rates are equal and much smaller than the atomic relaxation rates (good cavity limit).

It is shown here that if the excited atoms are initially cold, the atomic recoil may strongly influence the steady-state operation of the ring laser. When the unidirectional solution dominates over the bidirectional solution, the unbalanced radiation pressure forces accelerate the atoms. The induced longitudinal atomic momentum affects the stability of the stationary solutions: on resonance, the unidirectional solution becomes unstable and the bidirectional solution stable, whereas by detuning the cavity mode from the atomic resonance, a pulsed regime occurs for positive detuning ($\omega_{1,2} > \omega_0$), with unidirectional lasing periodically in opposite directions, whereas the laser quenches for negative detuning ($\omega_{1,2} < \omega_0$).

4.2. Model

The ring laser model considered here is described in Section 2 and shown schematically in Fig. 1. In

contrast to the previous section, the atoms are now considered to be strongly pumped, so that $\Lambda \gg \Gamma_{\parallel}$ and $D^{eq} \approx -0.5$. In addition, we assume that no radiation fields are fed into the cavity i.e. $A_1^{eq} = A_2^{eq} = 0$. In what follows, we assume for simplicity that $\Gamma_{\perp} = \Lambda$. Relaxing this assumption does not change the results presented here qualitatively.

We note that Eqs. (7)–(9) combine to gives the momentum rate equation,

$$(\mathrm{d}/\mathrm{d}\tau)\left[\langle p\rangle + I_1 - I_2\right] = -\kappa\left[I_1 - I_2\right], \qquad (23)$$

where $I_{1,2} = |A_{1,2}|^2$. We assume an initially cold and unbunched ($b = 0$) atomic sample. Hence, when $I_1 = I_2$ the average recoil $\langle p\rangle$ remains zero.

4.3. Results

We now discuss the solution of Eqs. (3)–(9), for an initial system of cold, unbunched, completely inverted (i.e., $D_j(0) = D_{eq} = -1/2$) and unpolarised, $S_{1j}(0) = S_{2j}(0) = 0$, atoms.

4.3.1. Lasing neglecting recoil

Without recoil, the system admits two steady-state solutions: the unidirectional solution, $I_{1,2} = I_s(1 - 1/g)$ and $I_{2,1} = 0$, and the bidirectional solution, $I_1 = I_2 = (I_s/2)[1 - (1 + \sqrt{8g+1})/4g]$, where $I_s = \Lambda/4\rho\kappa$ is the saturation intensity value, $g = \alpha/\kappa$ is the gain to losses ratio and $\alpha = \rho\Lambda/(\Lambda^2 + \Delta^2)$ is the linear gain. A linear stability analysis has shown that, above threshold, i.e., for $g > 1$, the bidirectional solution is unstable while the unidirectional solution is stable [16]. However, since the ring laser is assumed to have no preferred direction, it can oscillate in either of the modes determined by initial fluctuations. A more general analysis of the laser without adiabatic elimination of the gain medium atomic variables, has shown [16] that under suitable conditions the unidirectional solution becomes unstable due to Hopf bifurcation and self-induced pulsations in both directions are observed.

4.3.2. Lasing including recoil

1. *Resonant case*: Fig. 6a shows the effect of atomic recoil on the temporal evolution of the intensities I_1 and I_2. Eqs. (3)–(9) have been integrated for $\Delta = 0$, $\Lambda = 10$, $\rho = 10$ and $\kappa = 0.1$. The initial field amplitudes are $A_{10} = 10^{-3} + \epsilon$ and $A_{20} = 10^{-3}$, with a slight difference $\epsilon = 10^{-18}$. We compare the complete solution with recoil (continuous lines) with the solution obtained when the atomic recoil is artificially suppressed ($\dot{p}_j = 0$, dashed lines). Without recoil, the two intensities are equal until they bifurcate: the first mode saturates, whereas the second mode cavity damps. We note that exchanging the initial conditions,

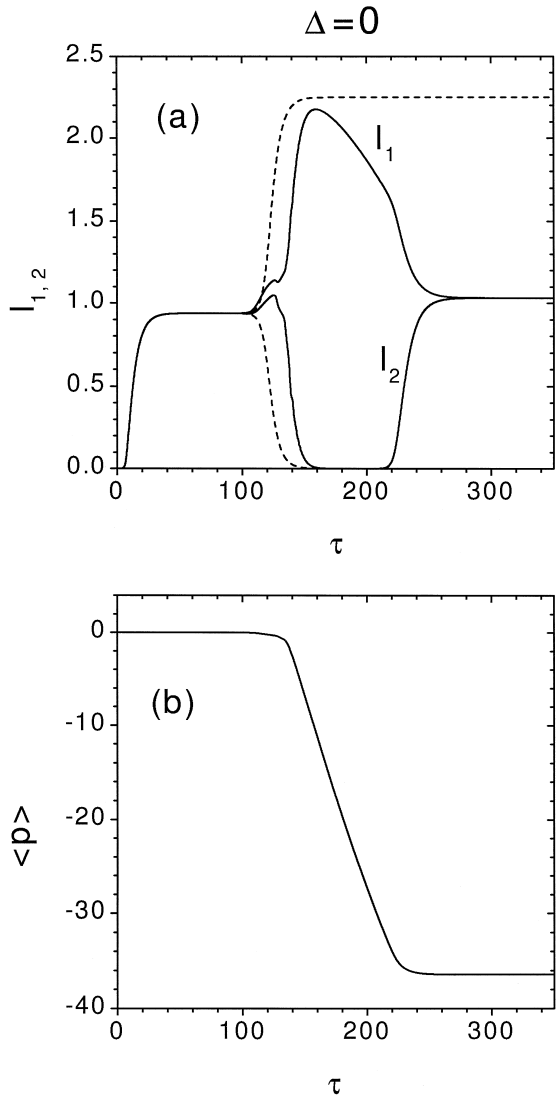

Fig. 6. Resonant ring laser: (a) scaled intensities I_1 and I_2 and (b) average momentum $\langle p\rangle$ versus τ for $\Delta = 0$, $\Lambda = 10$, $\rho = 10$, $\kappa = 0.1$, $A_{10} = 10^{-3} + \epsilon$, $A_{20} = 10^{-3}$ and $\epsilon = 10^{-18}$; dashed line in (a): solution where recoil has been artificially suppressed.

with I_2 slightly larger than I_1, their role is also exchanged, with I_2 saturating and I_1 damping. With recoil, the evolution of the fields is initially similar to that when recoil is neglected: there is a short period of bidirectional lasing followed by a bifurcation, after which I_1 grows to saturation and I_2 decays to zero. However for later times, atomic recoil changes the evolution of the laser modes significantly: I_1 decays and I_2 is amplified until $I_1 = I_2$. Therefore atomic recoil causes unidirectional lasing to be unstable and bidirectional lasing to be stable, in complete contrast to the situation when recoil is neglected. The bidirectional solution becomes stable when the average momentum $\langle p \rangle$, varying under the effect of the unbalanced radiation pressure forces during unidirectional operation, becomes sufficiently negative, as shown in Fig. 6b. To verify that this effect is due only to the radiation pressure, Eqs. (3)–(9) were solved numerically, with the atomic momentum p_j replaced by the average value $\langle p \rangle$ in Eqs. (3) and (4) and Eq. (23) used instead of Eq. (7). The results were unchanged, apart for some slight differences in the transient regime, proving that a sufficiently large average atomic velocity may stabilize the bidirectional solution.

2. *Blue-detuned cavity*: Fig. 7a shows the evolution of the laser modes for a blue-detuned case, with $\Delta = 10$, $\Lambda = 10$, $\rho = 20$, $\kappa = 0.1$. The initial field amplitudes are $A_{10} = 10^{-3} + \epsilon$ and $A_{20} = 10^{-3}$, with $\epsilon = 10^{-10}$. Neglecting recoil, the solution is similar to the resonant case shown in Fig. 6a, with the unidirectional solution stable and the bidirectional solution unstable. However when the effects of recoil are included, there is no steady-state and the system exhibits self-pulsations, with intensities periodically growing to the unidirectional saturation value and then damping. Fig. 7b shows the evolution of the average atomic momentum, $\langle p \rangle$, which also shows periodic oscillations.
3. *Red-detuned cavity*: Fig. 8a shows the behavior of the intensities of the two modes for a red-detuned case, with $\Delta = -10$ and the same other parameters as in Fig. 7. In this case, when $\langle p \rangle$ decreases (see Fig. 8b), the mode I_1 becomes unstable and decays after saturation, whereas I_2 remains unstable, so that lasing is suppressed in both modes.

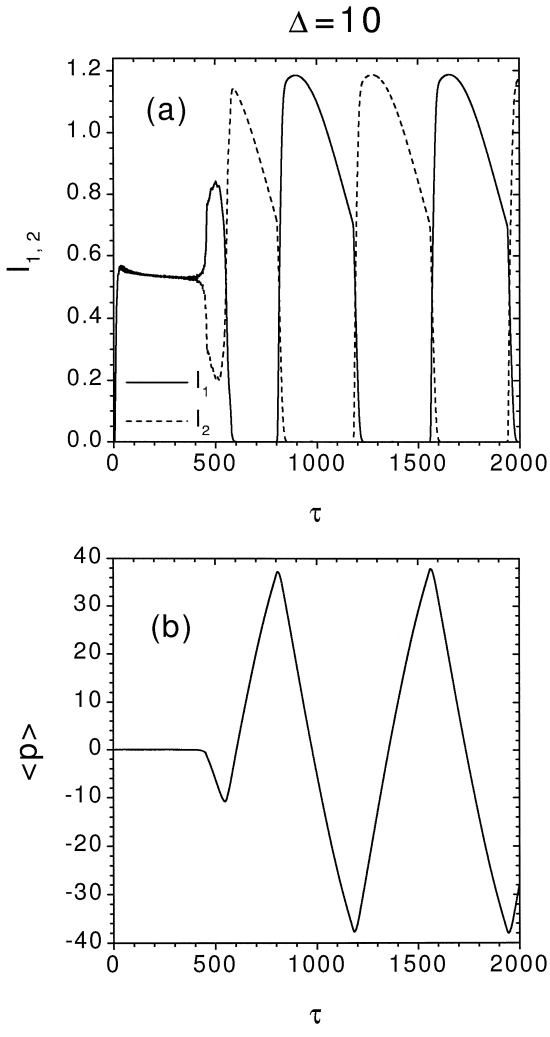

Fig. 7. Blue detuned ring laser: (a) scaled intensities I_1 and I_2 and (b) average momentum $\langle p \rangle$ versus τ for $\Delta = 10$, $\Lambda = 10$, $\rho = 20$, $\kappa = 0.1$, $A_{10} = 10^{-3} + \epsilon$, $A_{20} = 10^{-3}$ and $\epsilon = 10^{-10}$.

Another effect induced by atomic recoil is the formation of a transient density grating, due to the ponderomotive potential, created by the beat of the two counterpropagating radiation fields, which bunches the atoms. The bunching factor amplitude, $|b| = |\langle e^{-i\theta} \rangle|$, is shown in Fig. 9 for the three previous cases of Figs. 6–8, for (a) $\Delta = 0$, (b) $\Delta = 10$, and (c) $\Delta = -10$ until $\tau = 300$. In contrast to the case of optical bistability the density grating does not play a large role in the long-term evolution of the laser fields.

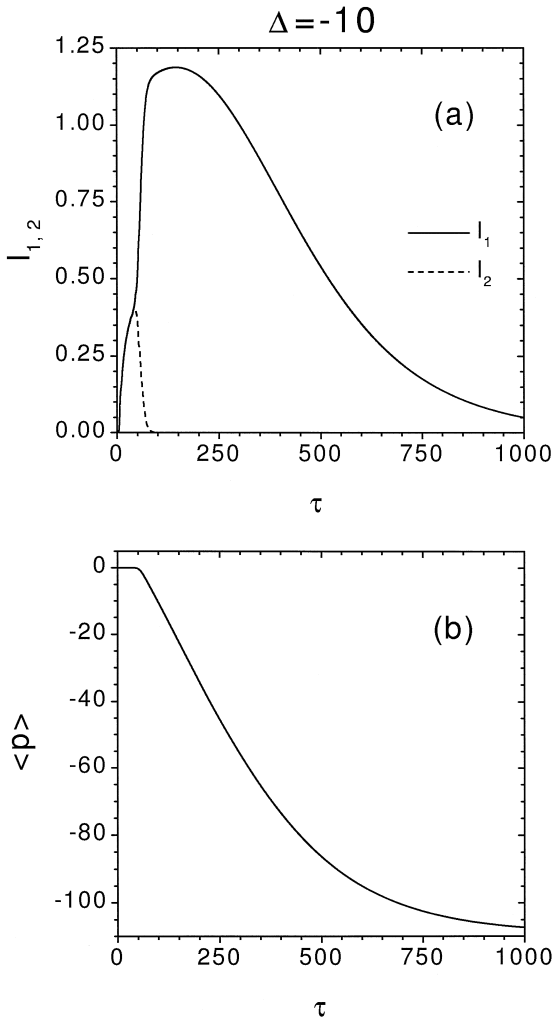

Fig. 8. Red-detuned ring laser: (a) scaled intensities I_1 and I_2 and (b) average momentum $\langle p \rangle$ versus τ for the same parameters as in Fig. 7, but with $\Delta = -10$.

4.4. Interpretation

A simple qualitative interpretation of these results may be given in terms of the Doppler shift due to the longitudinal momentum induced by radiation pressure. An atom moving with an axial velocity v_z effectively sees two different Doppler-shifted frequencies $\omega'_{1,2} = \omega(1 \mp v_z/c)$. The atom is resonant with radiation when these shifted frequencies coincide with the atomic resonance, that is, when $\omega_0 = \omega(1 \mp v_z/c)$. Consequently for large enough atomic velocities, two modes with equal frequencies in the laboratory frame may be widely separated in frequency in the rest frame of the atom.

1. *Resonant case*: When $\omega_0 = \omega$ (i.e., $\Delta = 0$), A_1 and A_2 are shifted from resonance by the same amount but in different directions, and hence experience equal gains $\alpha_1 = \alpha_2$, where $\alpha_{1,2} =$

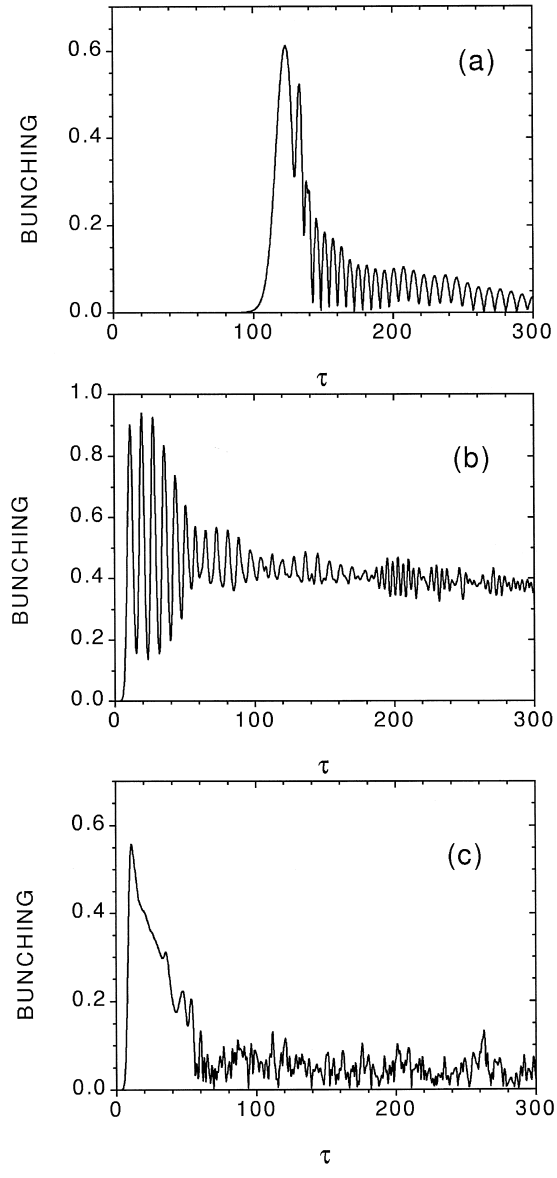

Fig. 9. Transient bunching factor amplitude $|b|$ versus τ for the cases of Figs. 6–8: (a): $\Delta = 0$; (b): $\Delta = 10$; (c): $\Delta = -10$.

$\rho\Lambda/(\Lambda^2+\Delta_{1,2}^2)$ and $\Delta_1=\Delta\mp\langle p\rangle/2$. The separation between the two line centres reduces the influence of one mode on the other, eventually making the two modes essentially uncoupled. This occurs approximately when the frequency difference between the line centres, ($|\langle p\rangle|$ in scaled notation), exceeds the gain linewidth, Λ. Fig. 6 shows that I_1 starts to decreases when $\langle p\rangle\approx-\Lambda$. Steady-state is possible when $\Delta=0$ because the average momentum is stationary when the intensities are equal, as stated by Eq. (23).

2. *Blue-detuned cavity*: For $\Delta>0$, the atomic momentum induced by radiation pressure Doppler shifts the frequency of the mode whose intensity is lower towards resonance (I_2 in the case of Fig. 8) increasing its gain, and pushes the other (more intense) mode further from resonance, decreasing its gain. The role of the two fields is exchanged when one intensity exceeds the other one, and the induced momentum changes sign. The result is a periodic behavior, with alternate growth and decay of the two intensities. The growing mode reaches its maximum when its effective frequency is resonant, i.e. when $|\langle p\rangle|=2\Delta$ (see Eqs. (3) and (4)): as can be seen in Fig. 7, where I_1 and I_2 are maxima when $\langle p\rangle\sim\pm20$, respectively.
3. *Red-detuned cavity*: Finally, for $\Delta<0$, the induced atomic momentum Doppler shifts the frequency of the mode with lower intensity further from resonance, preventing its growth. The other growing mode reaches a maximum when its Doppler-shifted frequency becomes resonant, i.e. for $\langle p\rangle\sim2\Delta$ in the case of Fig. 8. As the average momentum, $\langle p\rangle$, continues to increase due to the unbalanced radiation pressure force, the more intense mode is eventually driven out of resonance and decays to zero. Therefore for long times, both mode intensities decay to zero and laser operation is suppressed.

5. Conclusions

It has been shown theoretically that when describing atom-radiation interactions in passive and active cold, two-level atomic systems, the effect of atomic recoil can significantly change the nature of the interaction between the atoms and the radiation fields.

As an example involving a passive atomic system, we described absorptive optical bistability in a ring cavity containing cold atoms. When the effects of atomic recoil were included self-consistently, the lower branch of the bistability curve neglecting atomic motion could become unstable and the transmission switched to the upper branch i.e. the system was no longer truly bistable. This behaviour resulted from the simultaneous generation of an atomic density grating and a coherently backscattered radiation field. The formation of the density grating arose from a modulation of the radiation pressure forces exerted on the atoms. It should be noted that density grating formation has also been predicted in a system of cold atoms which have a predominantly dispersive interaction with the radiation field [1,2]. It could be expected therefore that dispersive optical bistability in a system of cold atoms would also be significantly affected by the inclusion of atomic recoil in the description of the interaction.

As an example involving an active atomic system, we described a bidirectional ring laser where the laser medium is a collection of cold atoms. Atomic recoil was shown to influence the stability of the steady-state operation of the ring laser. The usual unidirectional solution becomes unstable for a sufficiently large average atomic momentum is induced by the unbalanced radiation pressure forces. On resonance, the bidirectional solution is stable. Off resonance, the laser emits periodically in either direction when the detuning is positive and may suppress lasing in both directions when the detuning is negative. These results may form the basis for a method of avoiding strong mode competition in a homogeneously broadened bidirectional ring laser gyro tuned with the resonant atomic frequency of a cold gas system [17].

Acknowledgements

The authors would like to thank the Royal Society of Edinburgh and the EPSRC for support of GRMR and BM^{c}N respectively.

This paper is dedicated to Marlon Scully, whose friendship with one of us (R.B.) goes back more than 30 years.

References

[1] R. Bonifacio, L. De Salvo, Nucl. Instrum. Methods Phys. Res. A 341 (1994) 360; R. Bonifacio, L. De Salvo, L.M. Narducci, E.J. D'Angelo, Phys. Rev. A 50 (1994) 1716.
[2] R. Bonifacio, G.R.M. Robb, B.W.J. McNeil, Phys. Rev. A 56 (1997) 912, and refs. therein.
[3] M.G. Moore, P. Meystre, Phys. Rev. A 58 (1998) 3248.
[4] J. Guo, P.R. Berman, B. Dubetsky, P.R. Berman, Phys. Rev. A 46 (1992) 1426; B. Dubetsky, P.R. Berman, Phys. Rev. A 52 (1995) R2519.
[5] J.Y. Courtois, G. Grynberg, B. Louinis, P. Verkerk, Phys. Rev. Lett. 72 (1994) 3017; J.Y. Courtois, G. Grynberg, Adv. in Atomic, Mol. and Opt. Phys. 36 (1996) 87.
[6] P.R. Berman, Phys. Rev. A 59 (1999) 585.
[7] F.T. Arecchi, R. Bonifacio, IEEE J. Quantum Electron. 1 (1965) 169.
[8] R. Bonifacio, B.W.J. McNeil, G.R.M. Robb, Opt. Commun. 161 (1999) 1.
[9] R. Bonifacio, L. Lugiato, Opt. Commun. 19 (1976) 172.
[10] R. Bonifacio, L. Lugiato, Lett. Nuovo Cim. 21 (1978) 505.
[11] L. Lugiato, Progress in Optics XXI (1984) 69, and refs. therein.
[12] L. Desalvo, R. Cannerozzi, R. Bonifacio, E.J. D'Angelo, L.M. Narducci, Phys. Rev. A 52 (1995) 2342.
[13] See e.g. S. Stenholm, in: E. Arimondo, W.D. Phillips, F. Struma (Eds.), Proc. International School of Physics 'Enrico Fermi', course CXVIII, North-Holland, Amsterdam, 1992, p. 29.
[14] H. Zeghalche, P. Mandel, N.B. Abraham, L.M. Hoffer, G.L. Lippi, T. Mello, Phys. Rev. A 37 (1988) 470, and refs. therein.
[15] P. Meystre, M. Sargent III, Elements of Quantum Optics, Springer-Verlag, chap. 6.
[16] P. Mandel, G.P. Agrawal, Opt. Commun. 42 (1982) 269.
[17] L.N. Menegozzi, W.E. Lamb Jr., Phys. Rev. A 8 (1973) 2103.